Blöcher, G., Cacace, M., Reinsch, T., Watanabe, N. (2015): Evaluation of three exploitation concepts for a deep geothermal system in the North German Basin. - *Computers and Geosciences*, *82*, p. 120-129.

DOI: http://doi.org/10.1016/j.cageo.2015.06.005

Evaluation of three exploitation concepts for a deep geothermal system in the North German Basin

Guido Blöcher[a,*], Mauro Cacace[a], Thomas Reinsch[a], Norihiro Watanabe[b]

[a] *Helmholtz Centre Potsdam, GFZ German Research Centre for Geosciences, Telegrafenberg, 14473 Potsdam, Germany*
[b] *Helmholtz Centre for Environmental Research (UFZ), Permoserstr. 15, 04318 Leipzig, Germany*

Abstract

In this paper, we compare three exploitation strategies for the deep geothermal system of Groß Schönebeck in the North German Basin. Investigating optimum reservoir designs is one of the key issues for efficient and sustainable utilization of geothermal resource. With this objective we simulate the hydraulic-thermal coupled subsurface processes related to the provision of geothermal energy. The presented application including, visualization, mesh generation and numerical simulation is based on open source software. The numerical investigations of the three exploitation concepts take into account all geological layers, major natural fault zones, hydraulic fractures, geothermal wells and related hydraulic-thermal coupled processes. In the current exploitation concept, the fluid flows through the rock matrix between the injection and the production well (matrix dominated). The related numerical model is compared and calibrated to available field data. Then, the model is used to investigate two alternative stimulation concepts. All three concepts

*Corresponding author. Tel.: +49 331 288 1414; Fax: +49 331 288 1450. E-mail address: Guido.Bloecher@gfz-potsdam.de (G. Blöcher).

were evaluated taking into account the evolution of the production temperature as well as the hydraulic conductivity between production and injection well. As an alternative to the current situation, a fracture dominated system is investigated where the fluid flows through hydraulically induced fractures between injection and production well. Compared to the reference model, a twofold increase in productivity could be observed together with a significantly reduced time before the onset of a thermal breakthrough. The second alternative is a hybrid concept combining both matrix and fracture-dominated flow paths between the production and the injection well. We show that this hybrid approach could significantly increase the reservoir productivity and prolongs the time before the onset of thermal breakthrough.
Keywords: enhanced geothermal systems (EGS), numerical simulation, doublet system, faulted geological systems

1. Introduction

To reduce climate gas emissions, geothermal energy can play an important role for the future energy supply (Sims et al., 2007). Extracting energy from hot sedimentary aquifers may be considered as one of the most cost-effective energy sources with significantly reduced emissions compared to fossil fuels. The successful exploration, development and exploitation of geothermal resources is based on a collaborative effort involving different scientific and engineering disciplines. One of these disciplines is dynamic reservoir modeling which simulates the transient processes during the lifetime of the reservoir. This modeling is widely used to optimize the management and utilization geothermal resources.

To optimize exploitation strategy for geothermal resources we performed dynamic simulation based on geological information for the geothermal research site at Groß Schönebeck in the Northeast German Basin. This site is one of the key in-situ laboratories in Germany for the investigation of an efficient provision of geothermal energy from deep sedimentary basins. By means of the dynamic simulation we investigate three alternative exploitation concepts and we discuss advantages and disadvantages in terms of their productivity and sustainability. This means that productivity must be high enough and that a sufficient production temperature must be guaranteed for more than 30 years so that exploitation of geothermal energy can become part of the energy mix. A productivity index between 60 and 120 $m^3/(h * MPa)$ and a production temperature above 373 K is the requirement for efficient electricity generation (Hofmann et al., 2014).

The current state (reference model) represents the first exploitation concept (Figure 4b), there the fluid flows through the rock matrix. Field measurements indicate that this exploitation is not sufficient for economic use. Therefore, two additional exploitation concepts are considered: First, a fracture dominated system (Figure 5b) there the fluid flows through hydraulically induced fractures and second, a combination of matrix and fracture-dominated system (Figure 6b) referred to as hybrid-system in the following. The dynamic simulation of these three scenarios is based on an existing structural geological model (Moeck et al., 2008; Muñoz et al., 2010) and comprises heterogeneous geological layers, natural faults, induced fractures, and deviated geothermal wells (Figure 1).

The simulation of three alternative exploitation concepts for the Groß

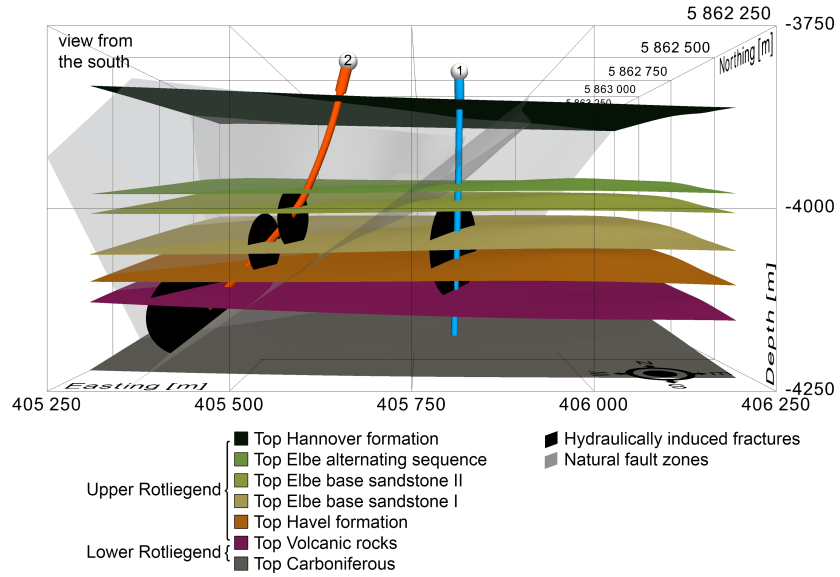

(a)

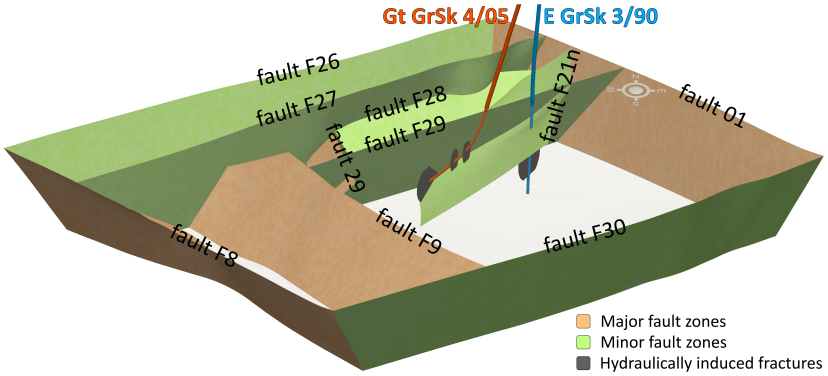

(b)

Figure 1: (a) Geological model developed on the basis of two-dimensional seismic and wellbore data. The injection well E GrSk 3/90 (1) is almost vertical and the production well Gt GrSk 4/05 A-2 (2) is directed towards a NE-striking/W-dipping fault. The black ellipses show the induced fractures of the doublet system at the Groß Schönebeck site (modified from Blöcher et al. (2010)). (b) Fault system of the Groß Schönebeck reservoir consisting of 130° striking major faults (hydraulic barriers), and 30° and 170° striking minor faults (hydraulically transmissive).

Schönebeck geothermal reservoir demonstrates how modeling is used to understand the current nature of the geothermal system (e.g., its properties and processes) and improve reservoir exploitation. Based on a validated reference model of the current state, we suggest an optimized well and stimulation design in terms of productivity and sustainability. The presented application (from structural geological model to complex reservoirs simulation) is based on open source software (Paraview[1] for visualisation, MeshIt (Cacace and Blöcher, 2015) including Tetgen (Si, 2015) for mesh generation and OpenGeoSys[2] for coupled simulations), thus presenting a cost efficient and robust alternative to commercial software for the scientific community.

For complex numerical simulations, geometries of different spatial scales and dimensions have to be handled by the simulators. This requirement is fulfilled by superimposing lower dimensional elements onto higher dimensional elements (Figure 3b), which is called conformable meshing (Lo, 2014). To satisfy the continuity condition, fracture and wellbore elements must be located along boundaries of the rock matrix elements (Segura and Carol, 2004). Besides conformable meshing, the applied software MeshIt (Cacace and Blöcher, 2015) supports various 3D geological models as input and provides interfaces to different commercial and open-source multi-physics simulators.

In order to present the evaluated exploitation concepts in combination with the required technical effort, the following structure was chosen: First, we explain the geological setting and available field measurements of the Groß Schönebeck site which are used to construct and to calibrate the numerical

[1] http://www.paraview.org/
[2] http://www.opengeosys.org/

models. Second, we present the results of evaluating these three exploitation concepts and discuss these results in terms of productivity and temperature evolution.

2. Site description

All available data of the geology, wells, hydraulically induced fractures and fault zones including their hydraulic and thermal properties will be integrated in the numerical investigation. The developed reference model will be calibrated by available field measurements (Section 2.2) in terms of productivity and flow patterns.

2.1. Geological setting

Groß Schönebeck is located about 40 km north of Berlin, Germany. The investigated geothermal reservoir of Groß Schönebeck is located between -3830 and -4250 m true vertical depth subsea (TVDSS). The faulted reservoir rocks can be roughly classified into siliciclastic sedimentary rocks consisting of conglomerates, sandstones and siltstones (Upper Rotliegend) and andesitic volcanic rocks (Lower Rotliegend). The siliclastic rocks can be subdivided depending on their lithological properties into five formations (Blöcher et al., 2010). Of these five formations (Figure 1a), the Elbe base sandstones I and II are the most promising horizons for geothermal exploitation. They are characterized by a total thickness of approximately 100 m (-4000 to -4100 m TVDSS), a permeability locally higher than 1 mD (Trautwein, 2005; Trautwein and Huenges, 2005), a porosity of up to 10% (Huenges and Hurter, 2002), and a temperature of about 150°C (Wolfgramm et al., 2003). Hydraulic and thermal properties of all units and faults (Table 1 and Table

Table 1: Hydraulic properties (porosity ϕ and permeability k) and thermal properties (specific heat capacity c_s and thermal conductivity λ_s of the solid) of the reservoir units (Blöcher et al., 2010).

Unit	ϕ [%]	k [m^2]	c_s [$\frac{J}{kgK}$]	λ_s [$\frac{W}{mK}$]
1) Hannover formation	1	4.9E-17	920	1.91
2) Elbe alternating sequence	3	3.2E-16	920	1.94
3) Elbe base sandstone II	8	6.4E-16	920	3.1
4) Elbe base sandstone I	15	1.3E-15	920	3.18
5) Havel formation	0.1	9.9E-17	1000	3.0
6) Volcanic rocks	0.5	9.9E-17	1380	2.31

2) are based on previously published data (see Blöcher et al. (2010) and references therein).

The sub-horizontal reservoir rocks are cross-cut by several natural fault zones striking preferentially from 130° (major faults) to 30° and 170° (minor faults) (Moeck et al., 2009). Within the current stress field, the latter bear the highest ratio of shear to normal stress, and are in a critically stressed state within the sandstones and in a highly stressed state within the volcanic layer (Figure 1b). According to previous studies which indicate a structural relationship between potential fluid flow along and across faults and their state of stress (Barton et al., 1995; Ito and Zoback, 2000), minor faults in Groß Schönebeck are assumed to be hydraulically transmissive, and the major fault zones are expected to behave as hydraulic barriers (Figure 1b).

Table 2: Hydraulic properties (porosity ϕ, permeability k and aperture a) of fault zones and induced fractures.

	ϕ [%]	k [m^2]	a [m]
Major fault zones	100	1.0E-15	1.0E-04
Minor fault zones	100	1.0E-13	1.0E-02
Induced fractures	26	1.0E-10	1.0E-02

2.2. Well and stimulation design - hydraulic well tests

Circulation of geothermal water is maintained via a thermal water loop consisting of a well doublet system with an injection (E GrSk 3/90) and a production (Gt GrSk 4/05 A-2) well, which was copleted in 2007 (Figure 1a). The geothermal water loop was established in 2011 by additional surface flow lines (Frick et al., 2011).

The injection well is an abandoned gas exploration well, which was re-opened in 2001. The injection/production potential of the well was tested along the entire open hole section between -3799 m to -4228 m TVDSS. The production potential of a well can be indicated by the productivity index (PI) which is defined as the flow rate per unit pressure drop $PI = \frac{\dot{V}}{\triangle p}$. The initial productivity index of the injection well was 0.97 $m^3/(h{*}MPa)$ (Zimmermann et al., 2009).

The production well Gt GrSk 4/05 A-2 was drilled along the minimal principal stress direction ($S_h = 288°$ azimuth) with an inclination of up to 49° (Zimmermann et al., 2010) and a total depth of 4404.4 m MD. Due to the inclination the horizontal distance of both wells is ranging between 300 and

450 m in the reservoir section. In such a doublet configuration, it is the rock matrix that is the heat exchanger, a system that we call matrix-dominated.

To increase the efficiency of the doublet system three stimulation treatments and eight perforation treatments were performed in the production well and four stimulation treatments were performed in the injection well, which is cased with a perforated liner within the reservoir (Figure 1a). At the production well, a water-frac treatment was applied in the low permeability volcanic rocks and two gel-proppant treatments were used to stimulate the sandstone sections (Zimmermann et al., 2010; Zimmermann and Reinicke, 2010). At the injection well, two gel-proppant fracs and two water-fracs were performed within the same reservoir section and are henceforth referred to as "multi-frac" (Zimmermann et al., 2009). Since all induced fractures are mainly tensile, they are parallel to the maximum horizontal stress direction $S_H = 18.5 \pm 3.7°$ (Kwiatek et al., 2010). The geometry of the individual fractures is summarised in Table 3. The horizontal distance between the water-frac, first gel-proppant frac and second gel-proppant frac within the production well and the multi-frac within the injection well is 448, 352, and 308 m, respectively (Blöcher et al., 2010). The hydraulic and geometric properties (Table 2) of the induced fractures are estimated using modeled data based on measured field data (Zimmermann and Reinicke, 2010).

To clean the well and to remove residual drilling mud in the near-wellbore vicinity, an acid matrix stimulation was performed in 2009 using a coil tubing unit (Zimmermann et al., 2011). To measure the magnitude of increase of the reservoir performance several production and injection tests were performed (Figure 2). After the stimulation treatments and before the acid

Table 3: Dimensions (half-length and height) of hydraulically induced fractures (Blöcher et al., 2010).

Frac type	Half-length $[m]$	Height $[m]$
Water-frac	190	175
Gel-proppant frac	60	95
Multi-frac	160	185

matrix stimulation, a casing lift test (CLT) in conjunction with flowmeter profiling (Figure 7) was carried out in 2007 to obtain hydraulic information from the production well. During this CLT, a fluid volume of 356 m^3 was produced during 11.8 h (Zimmermann et al., 2010). The calculated productivity index at the end of the test was 10.1 $m^3/(h*MPa)$. Following the acid matrix stimulation, an additional CLT was performed in 2009 indicating a productivity index of approximately 13-15 $m^3/(h*MPa)$ after producing a fluid volume of 140 m^3 in 4h (Zimmermann et al., 2011). After establishing the geothermal water loop, the reservoir was tested by the means of several communication experiments (CE, simultaneous injection and production). In the first of more than 100 CEs the productivity index was measured to be 6 $m^3/(h*MPa)$ for the production well. During this test a fluid volume of 141 m^3 was produced in 4.4 h.

None of the production tests reached steady state conditions (Figure 2). Therefore, the PI determined under such dynamic conditions must be considered to overestimate the real production potential of the reservoir. Additional field data also shows a further decrease in the overall productivity

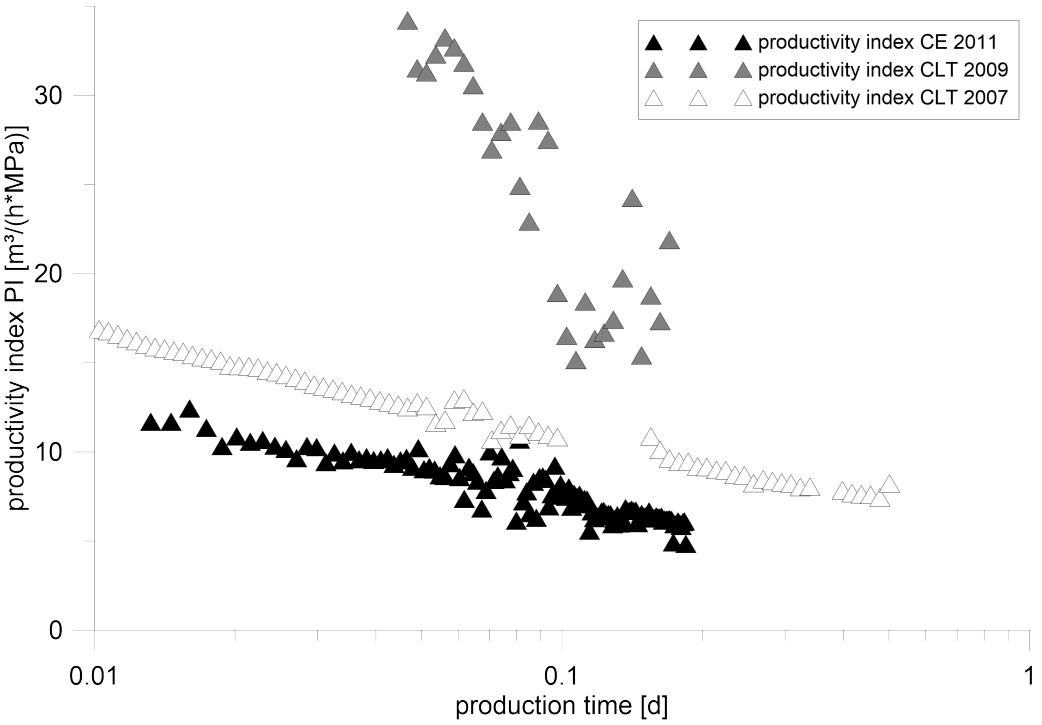

Figure 2: Time dependent behavior of the productivity index of the enhanced geothermal system Groß Schönebeck during the CLT 2007 (Zimmermann et al., 2010), CLT 2009 (Zimmermann et al., 2011) and CE in 2011.

of the reservoir from 6 $m^3/(h * MPa)$ in 2011 to 1 $m^3/(h * MPa)$ in 2013 (Blöcher et al., 2012).

3. Model setup

The reservoir models (see Figures 4, 5 and 6) used for hydraulic-thermal coupled simulations consist of 6 major geological formations, 10 fault zones, 4 to 6 hydraulic fractures (depending on the stimulation scenarios considered), and 2 to 3 geothermal wells (one production and two injection wells).

3.1. Meshing

Dynamic reservoir modeling requires a gridding or meshing of the 3D geological model. Commercial software exist which provide built-in modules to generate grids (e.g. EarthVision (Chen et al., 2013) and SKUA-GOCAD (e.g. Collon et al., 2015)) or unstructured meshes (Petrel (Souche et al., 2013)). The generated grids and meshes are generally used by related commercial simulators (e.g. Eclipse[3], NEXUS[4] or Paradigm SKUA-GOCAD and Flow Simulation[5]).

In this study all available geological information (geological layers, faults, fractures and wells) of the geothermal reservoir Groß Schönebeck have been converted from an existing EarthVision geo-model (Moeck et al., 2005) into a boundary-conforming, constrained Delaunay 3D mesh (Figure 3) by using the software MeshIt (Cacace and Blöcher, 2015). MeshIt is a multi-platform software, which combines algorithms from computational geometry and Delaunay triangulations within a graphical user interface. Geological information can be provided to MeshIt either in the form of volume-based 3D geological models (e.g. Paradigm Gocad [6], EarthVision[7] and Petrel[8]) for which existing importing interfaces exist (e.g. GoCad ASCII Files (*.gp)), or as single triplets surface files (x,y,z coordinates) which are provided by various 3D geological models. The assignment of specific material identi-

[3]http://www.software.slb.com/products/foundation/Pages/eclipse.aspx
[4] http://www.landmarksoftware.com/Pages/Nexus.aspx
[5]http://www.pdgm.com/Solutions.aspx
[6]http://www.pdgm.com/products/gocad/
[7]http://www.dgi.com/earthvision/evmain.html
[8]http://www.software.slb.com/products/platform/Pages/petrel.aspx

fiers (Figure 3a) to each component of the model, being a 3D matrix, 2D fault or 1D well element, enables to easily export the newly generated mesh to existing forward numerical simulators (e.g. OpenGeoSys[9] or Comsol[10]). Following this approach, source/sink points are represented by 0D points, geothermal wells by 1D poly-lines, faults and fractures by 2D triangulated surfaces, which are embedded in a 3D unstructured tetrahedral mesh of the rock matrix (Figure 3b).

For the three different exploitation scenarios the generated meshes consist of more than 4,180,000 tetrahedra. The typical time needed to build one of these meshes is approximately 1 min.

3.2. Numerical simulation

The hydraulic-thermal coupled simulations are conducted using OpenGeoSys (OGS) which is a scientific open-source initiative for numerical simulation of Thermo-Hydro-Mechanical-Chemical (THMC) processes in porous-fractured media (Watanabe et al., 2012; Kolditz et al., 2012). OGS is primarily based on the finite element method (FEM) and offers a hybrid approach combining discrete fracture and continua models for simulating flow, transport, and deformation processes in fractured rocks. In the following, governing equations used in the current study and applied numerical schemes are briefly presented.

With the Boussinesq approximation and Darcy's law (Equation 1), groundwater flow in porous media can be expressed as the following volume balance

[9] www.opengeosys.org

[10] www.comsol.com

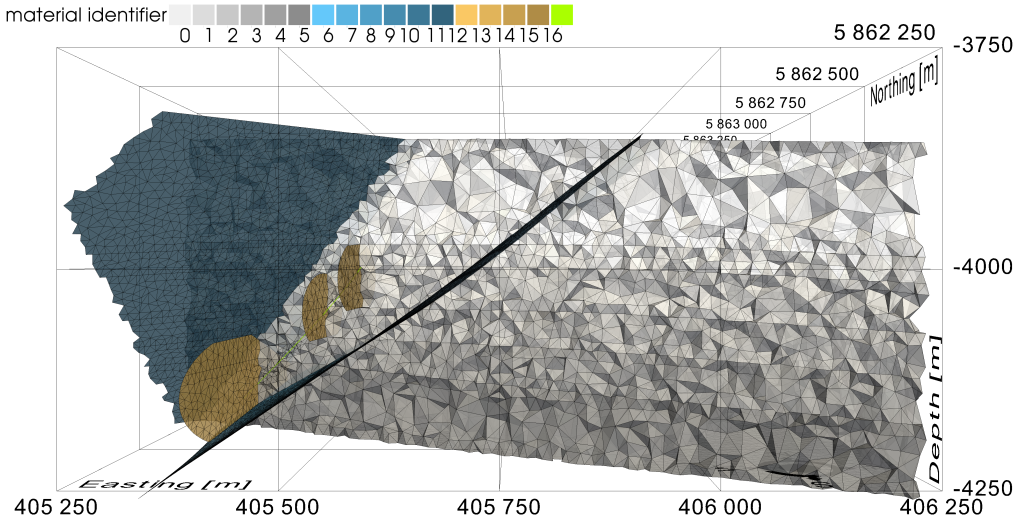

(a)

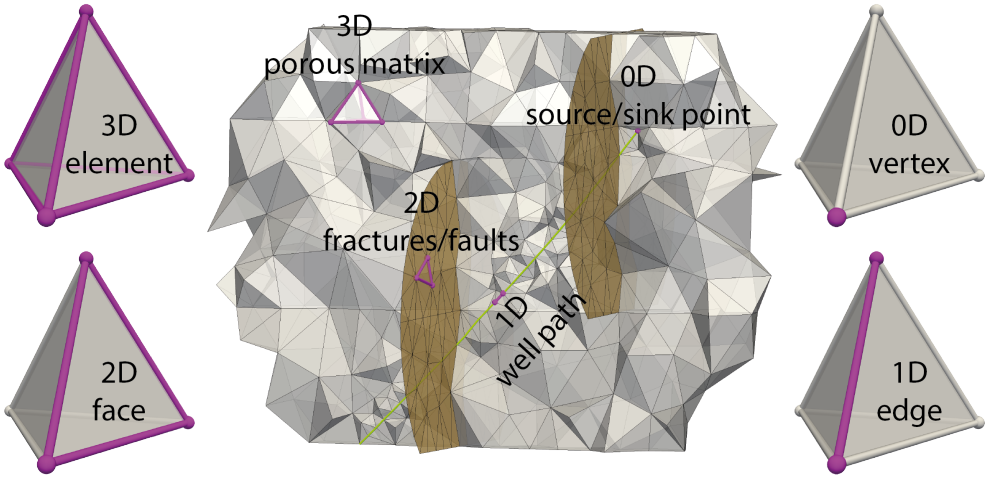

(b)

Figure 3: (a) Generated mesh of the reference case with specific material identifiers assigned to each component of the model, being a 3D matrix, 2D fault or 1D well element. (b) Detailed view of the production side: superposition of 0D (e.g. source/sink point), 1D (e.g. well path) and 2D (e.g. fractures/faults) elements onto 3D elements of the porous matrix.

equation (Lewis and Schrefler, 1998),

$$S_s \frac{\partial p}{\partial t} + \nabla \cdot \frac{\mathbf{k}}{\mu}(-\nabla p + \rho^l \mathbf{g}) = Q_H \tag{1}$$

where S_s is the constrained specific storage of the medium, p is liquid phase pressure, $\mathbf{k}$ is the permeability tensor, μ is fluid dynamic viscosity, ρ^l is the fluid density, $\mathbf{g}$ is the gravitational acceleration vector, and Q_H is a fluid source/sink term. For discrete fractures and wellbores, the permeability is given by the parallel plate concept (Snow, 1969) and the Hagen-Poiseuille equation, respectively.

Heat balance in porous media (Equation 2) can be expressed as (Lewis and Schrefler, 1998),

$$c_p \rho \frac{\partial T}{\partial t} + \nabla \cdot c_p^l \rho^l \mathbf{q}_H T - \lambda \nabla T = Q_T \tag{2}$$

where $c_p \rho = n c_p^l \rho^l + (1-n) c_p^s \rho^s$ is the heat storage of a porous medium with c_p^l specific heat capacity of the fluid, c_p^s specific heat capacity of the solid and ρ^s solid density. T is temperature, $\mathbf{q}_H$ is Darcy velocity, $\lambda = n\lambda^l + (1-n)\lambda^s$ is effective heat conductivity of the porous medium with λ^l heat conductivity of the fluid and λ^s heat conductivity of the solid, and Q_T is a source/sink term.

Details on the governing equations implemented in OGS are described in Watanabe et al. (2010, 2012) and references therein. Primary variables to be solved in the present non-linear multi-field problem are pressure and temperature. Galerkin FEM with linear interpolation and the backward Euler method are applied to obtain the approximated solutions.

To deal with the proposed reservoir representation including all 0D, 1D,

2D and 3D elements, two extensions have been made to OGS: (i) a monolithic approach for solving hydraulic-thermal (HT) coupled processes, and (ii) integration of the PETSc library for parallel computing. The monolithic approach means that the two equations for fluid flow and heat transport are solved simultaneously (Baca et al., 1984). Compared to the conventional partitioned coupling approach that solves the two equations separately, the monolithic approach provides more robust solutions for fully coupled hydraulic and heat transport processes. This is particularly important for geothermal reservoir simulations because heterogeneous flow fields are induced by the multi-dimensional elements. The Newton-Raphson method is used to solve the non-linear monolithic solution. Furthermore, in order to carry out the simulations in reasonable time (current time of computation is between 12 and 36 hours for 100 time steps), linear and nonlinear solvers of OGS are replaced by the PETSc library (Balay et al., 2014; Wang et al., 2014) to achieve efficient parallel computations based on MPI (Message Passing Interface) technology.

4. Simulations of exploitation concepts

We investigate the production temperature and pressure response of the reservoir for the three exploitation scenarios, namely a matrix-dominated, fracture-dominated, and hybrid system.

Firstly, a matrix-dominated system as established in the field at Groß Schönebeck has been simulated (Figure 4), and the results have been compared to available field data derived from the CLTs 2007 and 2009 and the CE 2011 experiments (Section 2.2). The numerical simulation of the matrix-

dominated system was calibrated with available geometrical and hydraulic data (Section 2.1). The calibrated model was afterwards used to numerically investigate the effects of considering fracture-dominated (Figure 5) and hybrid designs (Figure 6). For studying the latter ones, we integrated a third well path and additional hydraulic stimulations of the relevant wellbore sections into the model.

In the fracture-dominated design, we consider a direct connection between the former injection well E GrSk 3/90 and the planned well in the area of the volcanic rocks. Well connectivity is achieved by a water-frac treatment in the proposed well, which generates a common area of increased permeability between the two wells (Figure 5). In the hybrid design an additional gel-proppant treatment is considered in the Elbe base sandstone layer, thus connecting the former production well Gt GrSk 4/05 A-2 via the matrix to the newly established doublet system. In this configuration the proposed third well is assumed to act as production well, whereas the well E GrSk 3/90 and the well Gt GrSk 4/05 A-2 act as injection wells (Figure 6).

In all simulations, we consider a constant production rate of $\dot{V} = 30\ m^3/h$ and a desired production temperature of at least 400 K. The results are discussed in terms of the time required to approach quasi steady-state conditions, the transient PI and the time to thermal breakthrough. Here, the thermal breakthrough is defined as the time until the initial production temperature of 420 K drops below 400 K.

In all simulations, variations in fluid density and viscosity in response to changes in the temperature and pressure fields are considered, while the effects of variations of the salinity are neglected.

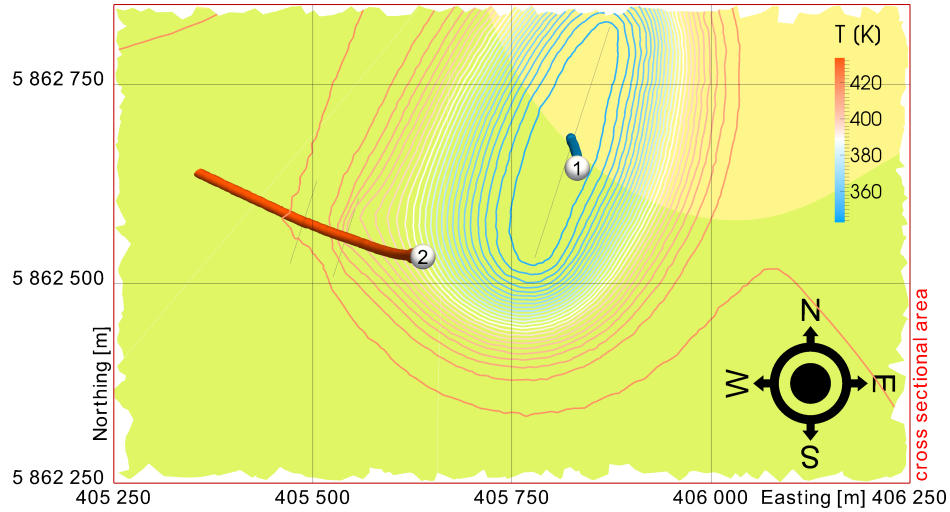

(a)

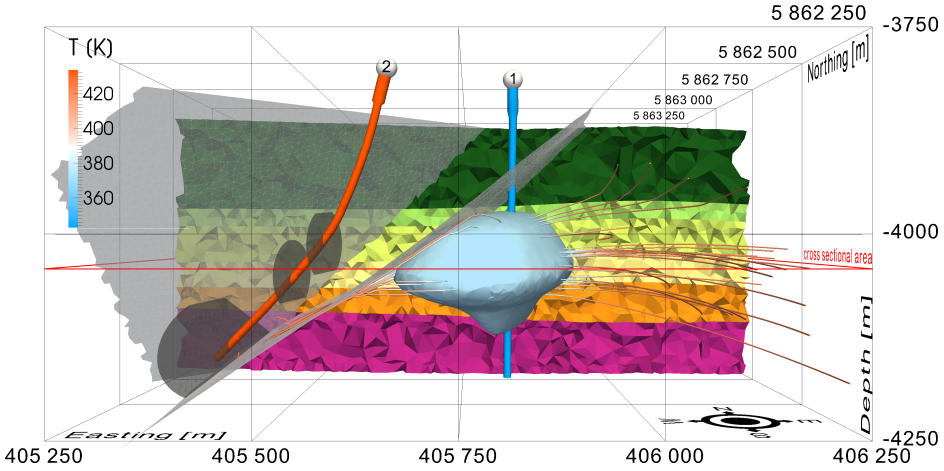

(b)

Figure 4: Matrix-dominated exploitation strategy consisting of one injection wells E GrSk 3/90 (1) and one production well Gt GrSk 4/05 A-2 (2) for the enhanced geothermal system Groß Schönebeck. Simulated temperature field after 30 years of production and injection of a horizontal cross section at -4042 m depth (a) and stream traces of the injected fluid including the corresponding 373.15 K isothermal surface in the reservoir section (b).

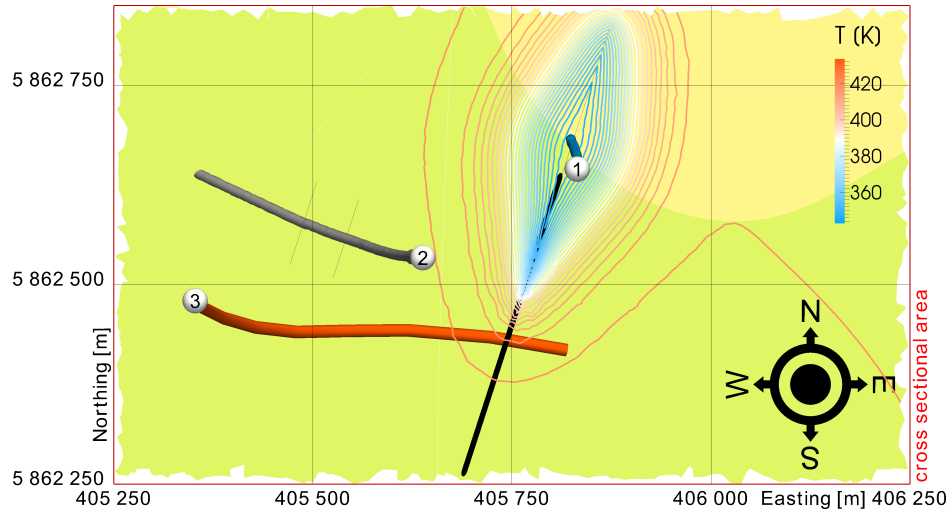

(a)

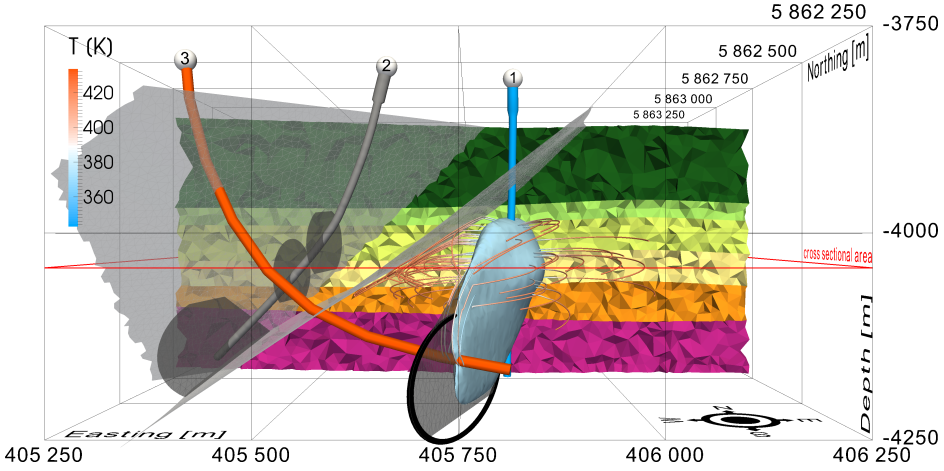

(b)

Figure 5: Fracture-dominated exploitation strategy consisting of one injection well E GrSk 3/90 (1), one planned production well (3) and one additional fracture (black ellipse) for the enhanced geothermal system Groß Schönebeck. Simulated temperature field after 30 years of production and injection of a horizontal cross section at -4042 m depth (a) and stream traces of the injected fluid including the corresponding 373.15 K isothermal surface in the reservoir section (b).

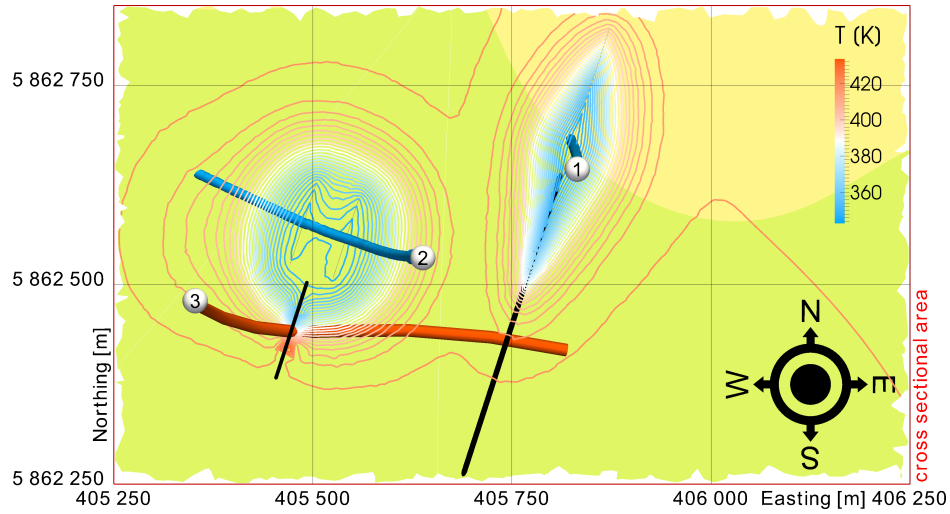

(a)

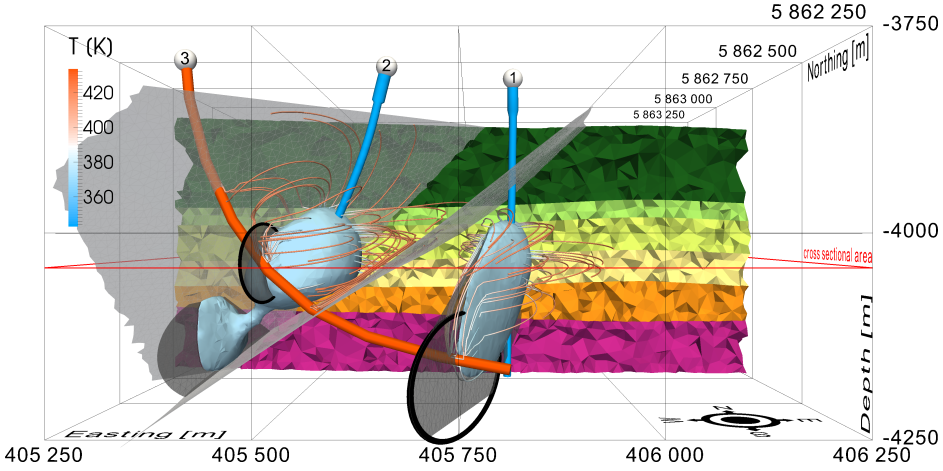

(b)

Figure 6: Hybrid exploitation strategy consisting of two injection wells E GrSk 3/90 (1) and Gt GrSk 4/05 A-2 (2), one planned production well (3) and two additional fractures (black ellipses) for the enhanced geothermal system Groß Schönebeck. Simulated temperature field after 30 years of production and injection of a horizontal cross section at -4042 m depth (a) and stream traces of the injected fluid including the corresponding 373.15 K isothermal surface in the reservoir section (b).

5. Results

5.1. Calibration of reference model

The simulation of the matrix-dominated exploitation strategy aims at reproducing the current exploitation conditions at the Groß Schönebeck research facility. To investigate the relevance of this simulation we compared the numerical results with results from the field experiments. Figure 7 shows the inflow profile of the production well Gt GrSk 4/05 A-2 obtained during the CLT 2007 in comparison to the simulated results. Although the simulation considers the well path as an open-hole section and the actual measured flow rate differed slightly from the simulated flow rate, an excellent fit between measured (Zimmermann et al., 2010; Henninges et al., 2012) and simulated contributions could be obtained. Differences can be observed below the second gel-proppant fracture, where the well is only partly perforated, and at the location of the fracture. At these positions turbulent flow conditions influence the measurements. In general, the cumulative flow should increase from bottom to top as shown by the simulation results. A cross-flow between different geological layers was not observed and is therefore considered to be improbable.

Besides the contribution of different intervals, the pressure response of the reservoir was simulated for the flow rates measured during the CLT 2007 (Zimmermann et al., 2010), the CLT 2009 (Zimmermann et al., 2011) as well as the CE 2011. Simulated results were compared to the measured reservoir pressure responses during these tests (see Section 2.2). For simulated and measured data, the productivity index was derived according to the production rate $\dot{V}$ and the corresponding pressure drawdown $\triangle p$. Since steady state

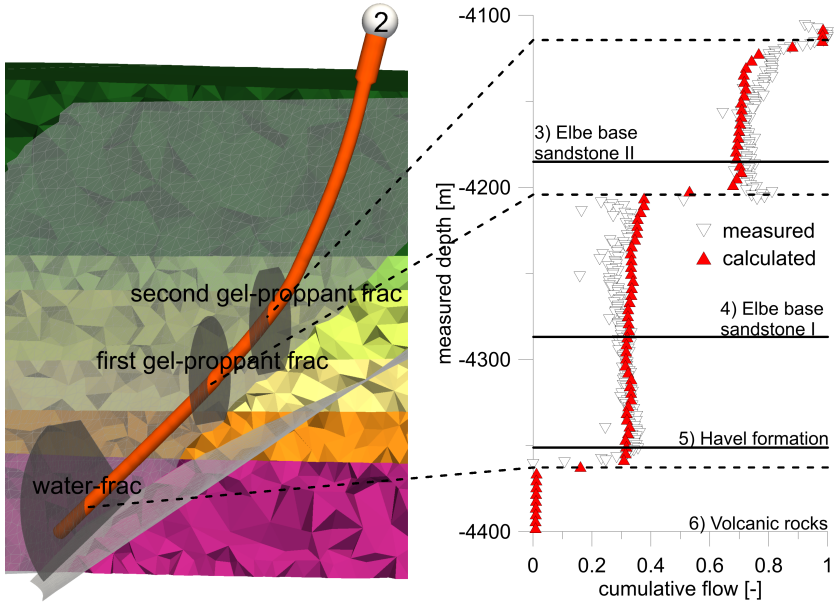

Figure 7: Measured (CLT 2007) and simulated inflow profile at the production well Gt GrSk 4/05 A-2 showing the individual contributions from the stimulated sections.

conditions were not reached during all field tests, we compare the evolution of the dynamic PI. For all tests, a linear dependency was observed between simulated and measured dynamic PI (Figure 8). For the CLT 2007 and the CE 2011 the measured PI is 1.5 to 2.5 times lower than the simulated one. For the CLT in 2009 a good match between measured and simulated PI is achieved.

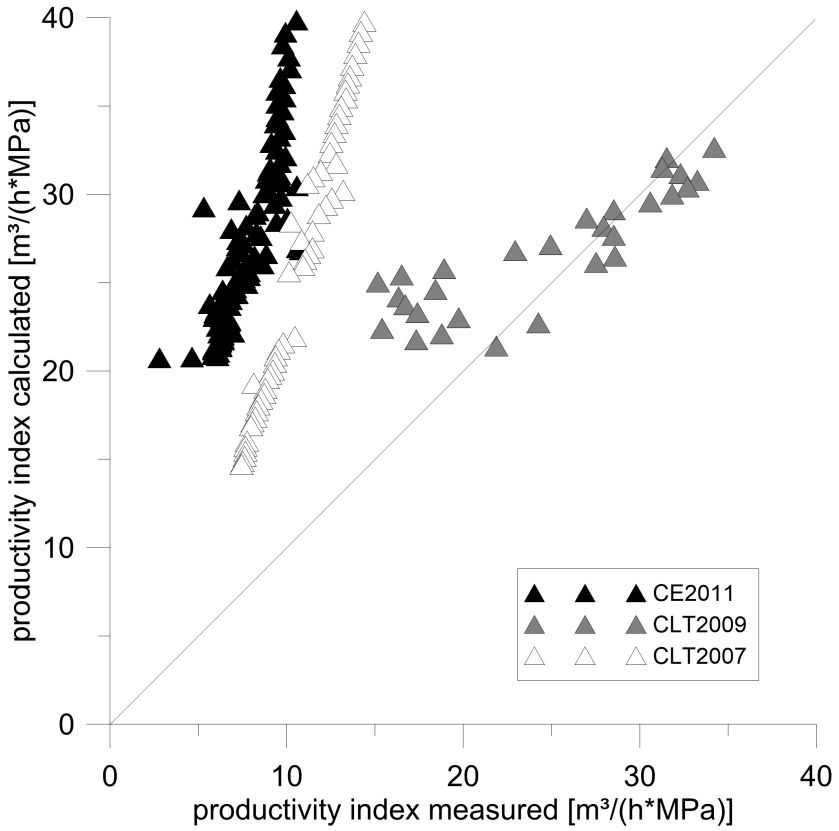

Figure 8: Measured and calculated productivity index. The dynamic productivity indexes calculated for the CLT 2007, CLT 2009 and CE 2011 are shown. The simulated values are based on the simulation of the matrix-dominated system.

Table 4: Simulation results obtained for the matrix-dominated, fracture-dominated and hybrid systems. Compared are the time for achieving hydraulic steady state conditions t_{ss}, the corresponding productivity index PI_{ss}, the onset time of thermal breakthrough t_{tb0}, and the time of thermal breakthrough t_{tb}.

Exploitation strategy	t_{ss} [years]	PI_{ss} $[m^3/(h*MPa)]$	t_{tb0} [years]	t_{tb} [years]
Matrix	1.56	3.65	24.14	>100
Fracture	0.14	8.11	0.78	3.73
Hybrid	0.44	11.19	2.13	12.55

5.2. Simulation of exploitation strategies

Based on the calibrated numerical simulation of the matrix-dominated system, the numerical simulations of the fracture-dominated and the hybrid system (Figure 5 and Figure 6) were adapted. The results of all three scenarios in terms of PI and temperature evolution are shown in Figure 9 and are summarized in Table 4.

For the matrix-dominated system (Figures 4a and 4b) quasi steady state conditions for the pressure field could be achieved after 1.56 years. Here quasi steady state is defined as minimum of the time derivative of the pressure field. The corresponding PI is 3.65 $m^3/(h*MPa)$. After 24.14 years, the temperature at the production well starts decreasing (more than 1 K temperature drop) but does not drop below 400 K after 100 years of production.

For the fracture-dominated system (Figures 5a and 5b) the production and injection points are only 290 m apart from each other and connected by a highly conductive hydraulic fracture. This has a positive effect on

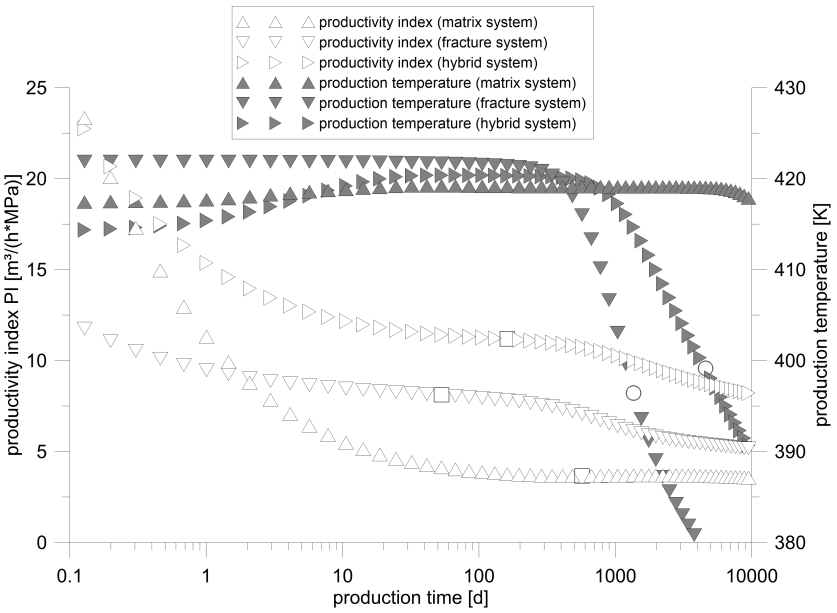

Figure 9: Time dependent behavior of productivity index and production temperature of a matrix-dominated, fracture-dominated and hybrid system, respectively. The squares and the circles indicate the time for achieving hydraulic steady state conditions and of thermal breakthrough, respectively.

the productivity but a negative effect on the temperature evolution of the production well. On one hand, steady state conditions are archived after 0.14 years and the corresponding productivity index is 8.11 $m^3/(h * MPa)$. On the other hand, thermal breakthrough starts after 0.78 years and the production temperature drops below 400 K after 3.73 years.

For the hybrid system (Figures 6a and 6b) the additional fracture in the sandstone layers increases the productivity. Furthermore, due to the increased accessible reservoir volume the time before thermal breakthrough in comparison to the fracture-dominated system is prolonged. By producing

30 m^3/h from the newly planned well while injecting 15 m^3/h each into E GrSk 3/90 and Gt GrSk 4/05 A-2, steady state conditions are achieved after 0.44 years and the corresponding PI is 11.19 $m^3/(h * MPa)$. Although the temperature starts decreasing after 2.13 years, a production temperature above 400 K can be expected for more than 12.5 years.

Comparing data from all three simulated scenarios (Figure 9), it can be seen that the initial PI (<0.1 days of production) is the highest for the matrix-dominated system followed by the hybrid and fracture-dominated systems. Comparing the wellbore and fracture storage, it is obvious that the matrix-dominated system has the highest storage followed by the hybrid and the fracture-dominated systems. Therefore, wellbore and fracture storage can be linked to the magnitude of the initial PI. Since fluid viscosity and density vary with pressure and temperature, all three simulations show a decrease of productivity after the onset of thermal breakthrough. An increased density and viscosity at the production side due to a thermal breakthrough will therefore reduce the simulated productivity.

6. Discussion and Conclusion

We have shown in this study that 3D modeling of a geothermal reservoir can bring valuable information for possible exploitation concepts. The current state, a matrix-dominated system, was compared to a fracture-dominated and a hybrid system. For the matrix-dominated system the sustainability of the production temperature could be proven. However, the relatively low PI of 3.65 $m^3/(h * MPa)$ does not allow an efficient utilization of the geothermal resource. The fracture-dominated system increases the PI by a factor of

more than 2. Due to a hydraulic short cut between production and injection well thermal breakthrough occurs in less than 4 years and the efficient and sustainable utilization is questionable. With an additional fracture along the production well, the productivity and the sustainability could be further improved.

6.1. Comparison of simulated and measured results from Groß Schönebeck

Data from the experiments performed in Groß Schönebeck were reproduced by the numerical simulation. The cumulative flow measured during the CLT 2007 is very similar to the simulation results, although the simulated and measured results slightly differ. Using the produced flow rate and comparing the simulated and measured pressure drawdown by means of the dynamic PI yields a linear relation between simulated and measured results. It is worth to mention that the CLT 2007 was performed before removing residual drilling mud (constituents: calcite, dolomite, and aragonite) from the wellbore vicinity (Zimmermann et al., 2011). A skin effect can therefore not be ruled out. After acidizing the reservoir interval (Section 3), the measured and simulated pressure response as shown for the CLT 2009 are in good agreement. During the following circulation experiments, a strong decrease in reservoir performance was observed (Regenspurg et al., 2015), indicating that additional effects influencing the well productivity must be considered.

6.2. Mechanical and chemical effects

Current field observations indicate that the productivity and sustainability of the Groß Schönebeck reservoir are influenced by several other processes which are not yet quantified. These processes might include: free gas and

two-phase flow, chemical precipitates in the wellbore, chemical alteration of the porous matrix, mechanical none sustainability of hydraulically induced fractures and barrier effects of internal fault zones (Regenspurg et al., 2015). These processes are currently not quantified and, therefore, not considered in the current evaluation of the exploitation concepts.

In particular, reactive transport can be simulated by coupling OGS to PhreeqC (Xie et al., 2006; Charlton and Parkhurst, 2011; Parkhurst and Appelo, 2013). Non-parallelization of this coupling results in more computational time. Integrating of two-phase flow (free gas phase within the brine) and internal no-flow boundaries (e.g. fault zones) into OGS is ongoing and will be considered as soon as available (Wang et al., 2011). The required fracture mechanics to show the sustainability of the induced fractures will be considered in future work. Since the mechanical processes are not fully coupled with the hydraulic-thermal coupled processes this feature was neglected. Not considering these effects will not change the general comparison of the exploitation strategies but will alter the prediction of productivity indices.

6.3. Workflow for reservoir simulations

In addition to direct application, the simulations conducted for Groß Schönebeck geothermal reservoir can be used as an example for transforming a structural geological model into a complex reservoir simulation. It can be applied to other settings including all geological features of interest. Furthermore, it provides a method for simulating groundwater and heat transport processes in a multi-component and multi-dimensional setting including 1D geothermal wells, 2D fault zones and macro fractures embedded in the three dimensional volume of the porous reservoir. The added value of the

study stems from enabling the transfer of 3D geological datasets of varying complexities into numerical reservoir simulators to quantify the processes of interest.

7. Acknowledgments

This work has been performed in the framework of the GeoEn Phase 2 project and was funded by the Federal Ministry of Education and Research [BMBF, 03G0767A]. The authors are grateful to the two anonymous reviewers who greatly improved the manuscript.

References

Baca, R.G., Arnett, R.C., Langford, D.W., 1984. Modelling fluid flow in fractured-porous rock masses by finite-element techniques. International Journal for Numerical Methods in Fluids 4, 337–348.

Balay, S., Abhyankar, S., Adams, M.F., Brown, J., Brune, P., Buschelman, K., Eijkhout, V., Gropp, W.D., Kaushik, D., Knepley, M.G., McInnes, L.C., Rupp, K., Smith, B.F., Zhang, H., 2014. PETSc Web page. http://www.mcs.anl.gov/petsc.

Barton, C., Zoback, M., Moss, D., 1995. Fluid flow along potentially active faults in crystalline rock. Geology 23, 683–686. doi:10.1130/0091-7613(1995)023<0683:FFAPAF>2.3.CO;2.

Blöcher, G., Zimmermann, G., Moeck, I., Huenges, E., 2012. Groß Schönebeck (D) - Moving forward on the learning curve: lessons learned

from projects in the recent years from projects, in: International Conference on Enhanced Geothermal Systems (Freiburg, Germany).

Blöcher, M.G., Zimmermann, G., Moeck, I., Brandt, W., Hassanzadegan, A., Magri, F., 2010. 3D numerical modeling of hydrothermal processes during the lifetime of a deep geothermal reservoir. Geofluids 10, 406–421. doi:10.1111/j.1468-8123.2010.00284.x.

Cacace, M., Blöcher, G., 2015. MeshIt - a software for three dimensional volumetric meshing of complex faulted reservoirs. Environmental Earth Sciences , 1–19doi:10.1007/s12665-015-4537-x.

Charlton, S.R., Parkhurst, D.L., 2011. Modules based on the geochemical model phreeqc for use in scripting and programming languages. Computers & Geosciences 37, 1653–1663.

Chen, M., Buscheck, T., Wagoner, J., Sun, Y., White, J., Chiaramonte, L., Aines, R., 2013. Analysis of fault leakage from Leroy underground natural gas storage facility, Wyoming, USA. Hydrogeology Journal 21, 1429–1445. doi:10.1007/s10040-013-1020-1.

Collon, P., Steckiewicz-Laurent, W., Pellerin, J., Laurent, G., Caumon, G., Reichart, G., Vaute, L., 2015. 3D geomodelling combining implicit surfaces and Voronoi-based remeshing: A case study in the Lorraine Coal Basin (France) . Computers & Geosciences 77, 29 – 43. doi:http://dx.doi.org/10.1016/j.cageo.2015.01.009.

Frick, S., Regenspurg, S., Kranz, S., Milsch, H., Saadat, A., Francke, H., Brandt, W., Huenges, E., 2011. Geochemical and process engineering

challenges for geothermal power generation. Chemie Ingenieur Technik 83, 2093–2104. doi:10.1002/cite.201100131.

Henninges, J., Brandt, W., Erbas, K., Moeck, I., Saadat, A., Reinsch, T., Zimmermann, G., 2012. Downhole monitoring during hydraulic experiments at the in-situ geothermal lab Gross Schönebeck, in: Proceedings 37th Workshop on Geothermal Reservoir Engineering, Stanford, USA. pp. 51–56.

Hofmann, H., Blöcher, G., Börsing, N., Maronde, N., Pastrik, N., Zimmermann, G., 2014. Potential for enhanced geothermal systems in low permeability limestones stimulation strategies for the Western Malm karst (Bavaria) . Geothermics 51, 351 – 367. doi:http://dx.doi.org/10.1016/j.geothermics.2014.03.003.

Huenges, E., Hurter, S., 2002. In-situ Geothermielabor Gro Schönebeck 2000/2001 : Bohrarbeiten, Bohrlochmessungen, Hydraulik, Formationsfluide, Tonminerale. Scientific Technical Report 02/14. GeoForschungsZentrum Potsdam, Germany.

Ito, T., Zoback, M.D., 2000. Fracture permeability and in situ stress to 7 km depth in the KTB scientific drillhole. Geophysical Research Letters 27, 1045–1048. doi:10.1029/1999GL011068.

Kolditz, O., Görke, U.J., Shao, H., Wang, W., 2012. Thermo-Hydro-Mechanical-Chemical Processes in Porous Media. 1 ed., Springer Publishing Company, 391pp.

Kwiatek, G., Bohnhoff, M., Dresen, G., Schulze, A., Schulte, T., Zimmermann, G., Huenges, E., 2010. Microseismicity induced during fluid-injection: A case study from the geothermal site at Groß Schönebeck, North German Basin. Acta Geophysica 58, 995–1020. doi:10.2478/s11600-010-0032-7.

Lewis, R.W., Schrefler, B.A., 1998. The Finite Element Method in the Static and Dynamic Deformation and Consolidation of Porous Media (Second Edition). Wiley.

Lo, D.S., 2014. Finite Element Mesh Generation. CRC Press.

Moeck, I., Holl, H.G., Schandelmeier, H., 2005. 3D lithofacies model building of the Rotliegend sediments of the NE German Basin, in: AAPG International Conference & Exhibition (Paris France).

Moeck, I., Kwiatek, G., Zimmermann, G., 2009. Slip tendency analysis, fault reactivation potential and induced seismicity in a deep geothermal reservoir. Journal of Structural Geology 31, 1174 – 1182. doi:10.1016/j.jsg.2009.06.012.

Moeck, I., Schandelmeier, H., Holl, H.G., 2008. The stress regime in a rotliegend reservoir of the northeast german basin. International Journal of Earth Sciences ISSN: 1437–3254. doi:10.1007/s00531-008-0316-1.

Muñoz, G., Bauer, K., Moeck, I., Schulze, A., Ritter, O., 2010. Exploring the Groß Schönebeck (Germany) geothermal site using a statistical joint interpretation of magnetotelluric and seismic tomography models. Geothermics 39, 35 – 45. doi:http://dx.doi.org/10.1016/j.geothermics.2009.12.

004. The European I-GET Project: Integrated Geophysical Exploration Technologies for Deep Geothermal Reservoirs.

Parkhurst, D.L., Appelo, C.A.J., 2013. Description of input and examples for PHREEQC version 3–A computer program for speciation, batch-reaction, one-dimensional transport, and inverse geochemical calculations. volume 6 of *Techniques and Methods*. U.S. Geological Survey, 497pp.

Regenspurg, S., Feldbusch, E., Byrne, J., Deon, F., Driba, D.L., Henninges, J., Kappler, A., Naumann, R., Reinsch, T., Schubert, C., 2015. Mineral precipitation during production of geothermal fluid from a permian rotliegend reservoir. Geothermics 54, 122 – 135. doi:http://dx.doi.org/10.1016/j.geothermics.2015.01.003.

Segura, J.M., Carol, I., 2004. On zero-thickness interface elements for diffusion problems. International Journal for Numerical and Analytical Methods in Geomechanics 28, 947–962. doi:10.1002/nag.358.

Si, H., 2015. TetGen, a Delaunay-Based Quality Tetrahedral Mesh Generator. ACM Trans. Math. Softw. 41, 11:1–11:36. doi:10.1145/2629697.

Sims, R., Schock, R., Adegbululgbe, A., Fenhann, J., Konstantinaviciute, I., Moomaw, W., Nimir, H., Schlamadinger, B., Torres-Martínez, J., Turner, C., Uchiyama, Y., Vuori, S., Wamukonya, N., Zhang, X., 2007. Energy supply, in: Metz, B., Davidson, O.R., Bosch, P.R., Dave, R., Meyer, L.A. (Eds.), Climate Change 2007: Mitigation. Contribution of Working Group III to the Fourth Assessment Report of the Intergovernmental Panel on

513 Climate Change. Cambridge University Press, Cambridge, United King-
514 dom and New York, NY, USA, pp. 251–322.

515 Snow, D.T., 1969. Anisotropic permeability of fractured media. Water Re-
516 sources Research 5, 1273–1289.

517 Souche, L., Lepage, F., Iskenova, G., 2013. Volume based modeling - Auto-
518 mated construction of complex structural models, in: 75th EAGE Confer-
519 ence & Exhibition incorporating SPE EUROPEC 2013 London, UK, 10-13
520 June 2013.

521 Trautwein, U., 2005. Poroelastische Verformung und petrophysikalische
522 Eigenschaften von Rotliegend Sandsteinen. Ph.D. thesis. Technische Uni-
523 versität Berlin.

524 Trautwein, U., Huenges, E., 2005. Poroelastic behaviour of physical proper-
525 ties in rotliegend sandstones under uniaxial strain. International Journal
526 of Rock Mechanics and Mining Sciences 42, 7–8, 924–932.

527 Wang, W., Fischer, T., Zehner, B., Böttcher, N., Görke, U.J., Kolditz, O.,
528 2014. A parallel finite element method for two-phase flow processes in
529 porous media: Opengeosys with petsc. Environmental Earth Sciences ,
530 1–17doi:10.1007/s12665-014-3576-z.

531 Wang, W., Rutqvist, J., Grke, U.J., Birkholzer, J., Kolditz, O., 2011. Non-
532 isothermal flow in low permeable porous media: a comparison of richards
533 and two-phase flow approaches. Environmental Earth Sciences 62, 1197–
534 1207. doi:10.1007/s12665-010-0608-1.

Watanabe, N., Wang, W., McDermott, C., Taniguchi, T., Kolditz, O., 2010. Uncertainty analysis of thermo-hydro-mechanical coupled processes in heterogeneous porous media. Computational Mechanics 45, 263–280. doi:10.1007/s00466-009-0445-9.

Watanabe, N., Wang, W., Taron, J., Görke, U.J., Kolditz, O., 2012. Lower-dimensional interface elements with local enrichment: application to coupled hydro-mechanical problems in discretely fractured porous media. International Journal for Numerical Methods in Engineering 90, 1010–1034. doi:10.1002/nme.3353.

Wolfgramm, M., Seibt, A., Hurter, S., Zimmermann, G., 2003. Origin of geothermal fluids of permo-carboniferous rocks in the ne german basin (ne germany). Journal of Geochemical Exploration 78–79, 127–131. doi:DOI:10.1016/S0375-6742(03)00133-X.

Xie, M., Bauer, S., Kolditz, O., Nowak, T., Shao, H., 2006. Numerical simulation of reactive processes in an experiment with partially saturated bentonite. Journal of Contaminant Hydrology 83, 122 – 147. doi:http://dx.doi.org/10.1016/j.jconhyd.2005.11.003.

Zimmermann, G., Blöcher, G., Reinicke, A., Brandt, W., 2011. Rock specific hydraulic fracturing and matrix acidizing to enhance a geothermal system Concepts and field results. Tectonophysics 503, 146 – 154. doi:10.1016/j.tecto.2010.09.026.

Zimmermann, G., Moeck, I., Blöcher, G., 2010. Cyclic waterfrac stimulation to develop an Enhanced Geothermal System (EGS) - Conceptual

558 design and experimental results. Geothermics 39, 59–69. doi:10.1016/j.
559 geothermics.2009.10.003.

560 Zimmermann, G., Reinicke, A., 2010. Hydraulic stimulation of a deep
561 sandstone reservoir to develop an Enhanced Geothermal System: Labo-
562 ratory and field experiments. Geothermics 39, 70 – 77. doi:10.1016/j.
563 geothermics.2009.12.003.

564 Zimmermann, G., Tischner, T., Legarth, B., Huenges, E., 2009. Pressure-
565 dependent production efficiency of an Enhanced Geothermal System
566 (EGS): Stimulation results and implications for hydraulic fracture treat-
567 ments. Pure and Applied Geophysics 166, 1089–1106. doi:10.1007/
568 s00024-009-0482-5.

List of Figures

List of Tables